DOI: 10.31401/WS.2024.proc.07

Moderate Magnetic Storm Expected as a Typical Space Weather Event in the Era of the Decreased Solar Activity

Gromova L.I.[1], Kleimenova N.G.[2], Gromov S.V.[1], Malysheva L.M.[2]

[1]IZMIRAN, Moscow, Troitsk, Russia; gromova@izmiran.ru
[2]Schmidt Institute of Physics of the Earth RAS, Moscow, Russia

Abstract

The 25th cycle of solar activity (SA) is the second one in the epoch of decreased SA when the geomagnetic activity become lower year by year. Really, the number of intense magnetic storms in the 23rd, 24th, and approaching its maximum in the 25th SA cycle is decreased. Thus, moderate magnetic storms (50 < |*SymH*| <100 nT or G2-storms) become the most expected events of the space weather. Here we discuss the behavior of the magnetic storm on September 12, 2023 as an example of a typical moderate magnetic storm. Our study was based on the analysis of the global maps of ionospheric and field-aligned currents obtained from magnetic measurements on 66 low-orbit AMPERE project satellites and electrons and ions data from DMSP satellites as well as the ground-based magnetic data from the Scandinavian IMAGE profile and Intermagnet. It was shown that the initial phase of the magnetic storm was characterized by daytime polar-latitude geomagnetic disturbances and the storm main phase was associated with nighttime substorms in auroral latitudes accompanied by positive magnetic bays at the middle latitudes. It was supposed that such magnetic storms caused by both magnetic clouds or high-speed streams from coronal holes, could be the most expected phenomena in the near future.

Keywords: Solar activity; Magnetic storm; Substorm.

Introduction

The current 25th cycle of the solar activity is the second cycle in the era of decreased solar activity, which, according to forecasts, can last until the mid-70s of the 21st century [Ishkov, 2023]. During such an era, the level of geomagnetic activity decreases and the number of intense magnetic storms reduces. As it is shown in [Selvakumaran et al., 2016] the reduced geoeffectiveness in the solar cycle 24 comparing to the cycle 23 occurs mainly due to the decrease in the intense storms and to a smaller extent in the number of moderate storms. A decrease in the number of intense magnetic storms is also noted in 25th cycle that is demonstrated in Table 1 from [Gopalswamy et al., 2023].

Table 1. *Number of intense storms during the first 41 months of solar cycles 23-25.*

Solar Cycle	#CME storms	#CIR Storms	Total
SC 23	18	3	21 (18)[1]
SC 24	5	0	5 (0)
SC25	4	0	4 (1)

[1]The numbers in the parentheses of this column correspond to the rise phase.

The days with magnetic storms decreased from cycle to cycle and the proportion of days of moderate magnetic storms increased, for example, see as it is shown in Figure 1.

Thus, we could expect that *moderate* magnetic storms may be the most typical space weather events in an era of decreased solar activity.

The aim of our work is to study the spatiotemporal distribution of substorm geomagnetic disturbances during the typical *moderate* magnetic storm as a storm which may be the most expected event at an early date. For our study we chose the magnetic storm on September 12, 2023.

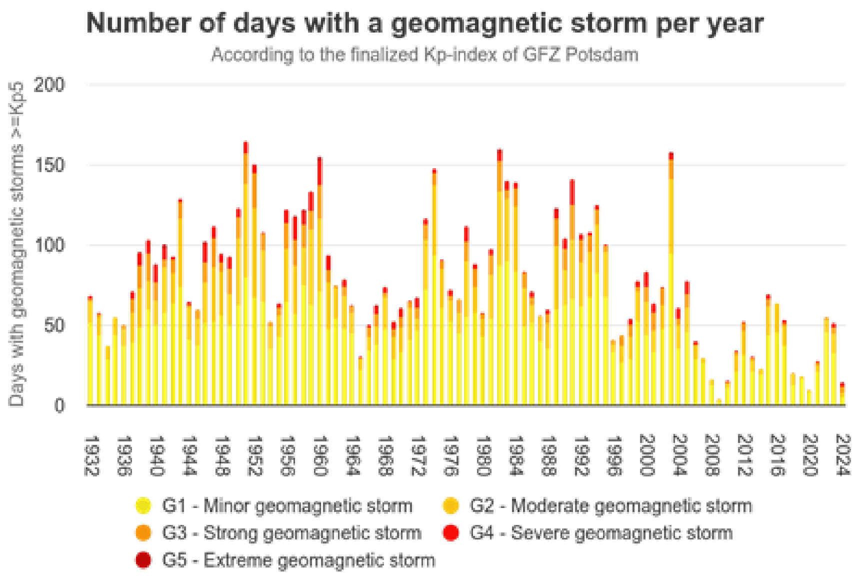

***Figure 1**. Number storm days in 20-25th solar activity cycles.*
From https://www.spaceweatherlive.com

Data

In our study we used the ground-based magnetic data from the Scandinavian IMAGE (https://space.fmi.fi/image/) and Intermagnet (https://imag-data.bgs.ac.uk/GIN_V1/) networks, as well as global maps of ionospheric and field-aligned currents obtained from AMPERE project (https://ampere.jhuapl.edu/) and electrons and ions data from DMSP (https://dmsp.bc.edu/).

AMPERE project is based on simultaneous magnetic measurements on 66 low-orbit satellites. The processing of the satellite data averaged over a 10-minute interval allows to analyze the global distribution of ionospheric and field-aligned currents. The maps are generated at 2-minute intervals. We assign each map to the middle of the averaging 10-min interval. Note, that AMPERE satellite data can represent the real planetary distribution of geomagnetic activity, which we cannot derive from ground-based data, since the stations are unevenly spaced due to large ocean expanses, and/or due to the lack of observation points (for example, in Siberia).

Variation of the Interplanetary Magnetic Field (IMF) and the solar wind parameters were proceeded from OMNI database http://omniweb.gsfc.nasa.gov, *PCN*-index values were obtained from http://pcindex.org.

We studied substorm activity in the magnetic storm basing on the analysis of the *AL*-index data from http://wdc.kugi.kyoto-u.ac.jp.

Magnetic storm on September 12, 2023

This *moderate* magnetic storm (G2, Kp_{max} = 5+) was noted as a response of the passage of three consecutive high-speed streams of the solar wind from coronal holes. [https://www.izmiran.ru/services/saf/archive/]. It was preceded by a long magnetically quiet period (Figure 2).

As it is shown in Figure 3 the magnetic storm began after the SC with a short (~3 hours) initial phase, when the solar wind dynamic pressure *Psw* (speed *V*, density *Np*) increased significantly, and the IMF components *Bz* and *By* varied slightly and remained negative. After

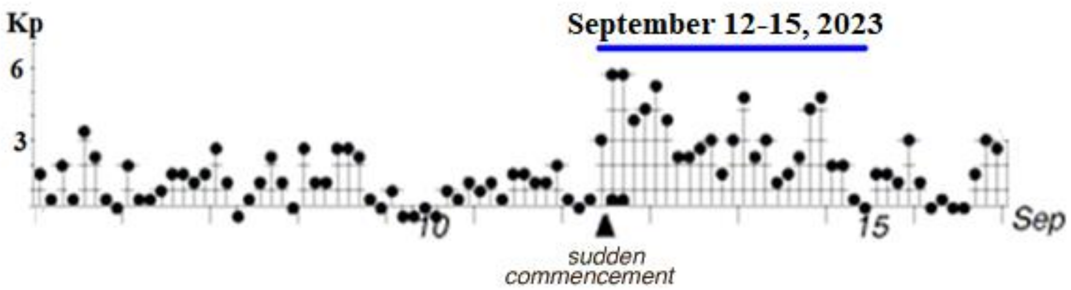

Figure 2. *Geomagnetic activity on September 6 – 16, 2023 by Kp-index. From https://kp.gfz-potsdam.de*

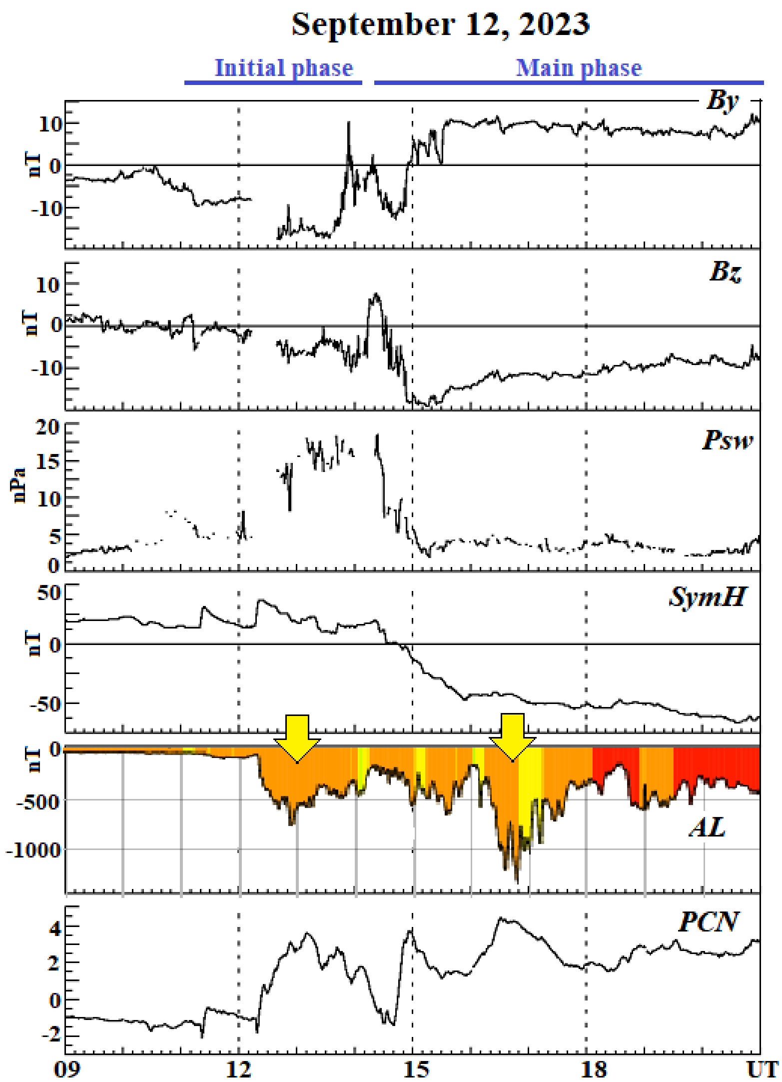

Figure 3. *The variation of the IMF and solar wind parameters, planetary indices SymH – index of the storm, Al - index of the auroral activity and PCN –index of geomagnetic activity in the Northern polar cap. Yellow arrows point the substorms under consideration.*

a sharp positive impulse and a rapid drop of the IMF *Bz* component and a simultaneous sharp decreasing of *Psw*, the main phase of the storm began and developed under the gradually decreasing negative IMF *Bz*, positive IMF *By* and a consistently small *Psw*.

Magnetic storms are typically accompanied by substorms [Akasofu and Chapman, 1963], and stronger storm are accompanied by more intense substorms [Feldstein et al., 1997], due to the southern component of the interplanetary magnetic field (the IMF *Bz* < 0) as both phenomena cause. As it is seen in Figure 3 the IMF *Bz* was negative both in the initial and main phase of the magnetic storm.

In the initial phase of the magnetic storm, one can observed the isolated substorm with *AL*–index-about -750 nT (~13:00 UT). During the main phase, which began with a sharp drop in the values of the southern IMF *Bz* component till -20 nT, an intense substorm was observed with *AL*-index -1400 nT (~16:50 UT). An increase in the *PCN*-index before each substorm indicates the increasing input of energy from the solar wind into the magnetosphere.

Thus, unexpectedly the considered *moderate* magnetic storm was accompanied by *high* substorm activity.

Substorm development in the initial and main phases of the magnetic storm

Figure 4 shows magnetograms of stations where we observed substorm development in the initial and main phase of the storm. Figure 4a shows the data from Scandinavian meridian

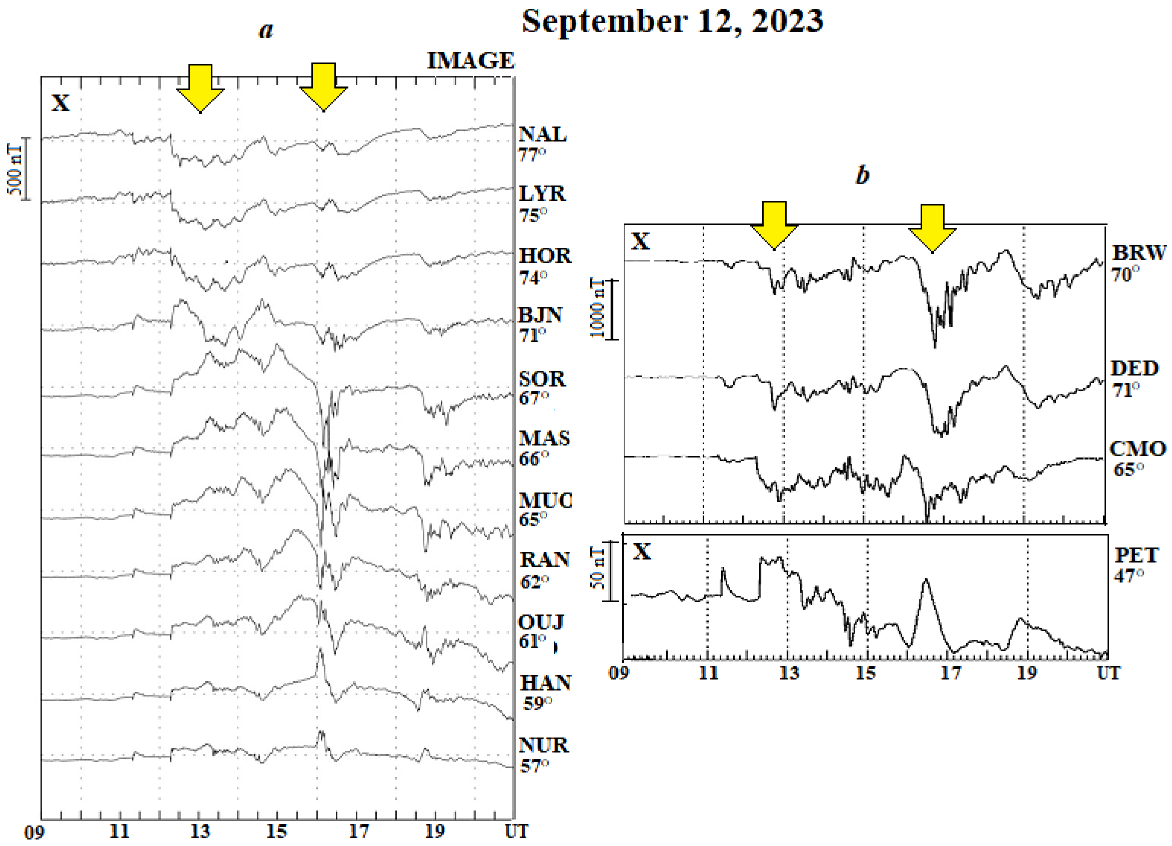

Figure 4. *Magnetograms of IMAGE profile stations (a) and high latitude stations of American sector and Russian mid latitude stastion PET (b). Yellow arrows point the substorms under consideration.*

profile of IMAGE network located the same longitudinal sector at MLAT 57-78°, approximately at the same longitude, MLT = UT+2.7. In Figure 4b one can see the magnetograms from some high-latitudes stations of the American sector: BRW (70°, MLT =

UT-12), DED (71°, MLT = UT-11), CMO (65°, MLT = UT-10), and from Russian mid-latitude station PET (47°, MLT=UT-14) located approximately near this longitudinal sector.

Global distributions of the eastward and westward electrojets and field-aligned currents and spectrograms of DMSP in the maximum of the substorm in the initial (~13:00 UT) and main phase (~16:40 UT) of the magnetic storm are demonstrated in Figure 5 and Figure 6 correspondingly.

The dayside disturbances in the initial storm phase

In the initial phase of the storm, the daytime negative magnetic bays were observed in the *X*-component of the geomagnetic field, were recorded at some polar stations in Scandinavia (Figure 4a). These bays were accompanied by the precipitation of electrons and ions into the ionosphere (Figure 5c) and counterclockwise ionospheric vortex in the afternoon sector. One can see the development of an eastward electrojet i.e. increasing of the upward field-aligned currents (Figure 5b) in the same sector of the high latitudes.

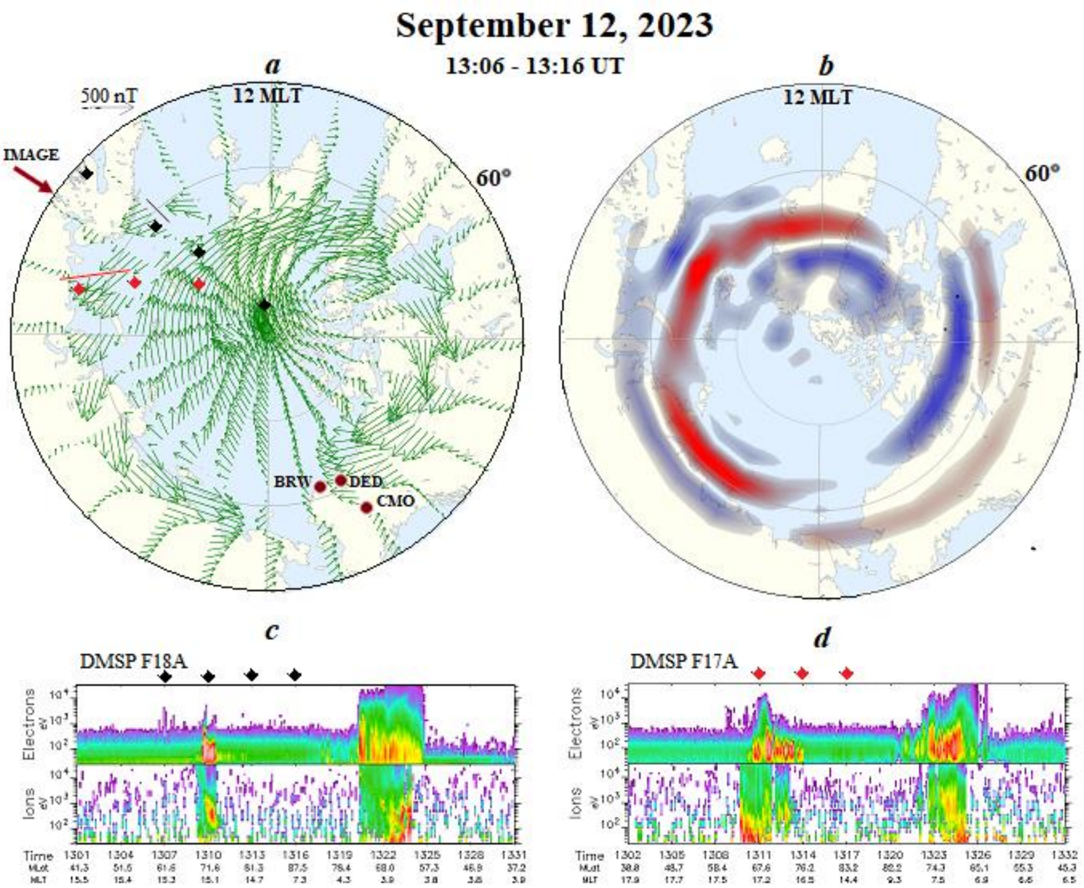

Figure 5. *AMPERE maps electrojets (a) and field-aligned currents (b) in the maximum of intensity of the substorm in the initial phase of the storm; spectrograms of DMSP F18A (c) and F17A (d) during the considered interval. Red arrow point the IMAGE meridian, red circles point the location of the station of American sector, rhombus (black one for F18A, red one for F17A) on the maps mark satellite passes, thin lines show approximate area of particle precipitation measured by DMSP.*

At the same time, in the early morning sector, a substorm developed at MLAT-latitudes ~65°, accompanied by positive bays at mid-latitudes (Figure 4b). This is evidence of the formation of substorm current wedge, which is one of the main features of substorm development [Kepko et al, 2015].

The substorms in the main storm phase

During the main phase of the magnetic storm, the intense magnetospheric substorm was observed in the post-midnight sector of the auroral latitudes (BRW, DED, CMO). One can see strong eastward electrojet and the development of positive mid-latitude magnetic bays as well as an intensification of the morning clockwise vortex, i.e. enhancement of field-aligned currents, that is typical for the development of very intense substorms and supersubstorms.

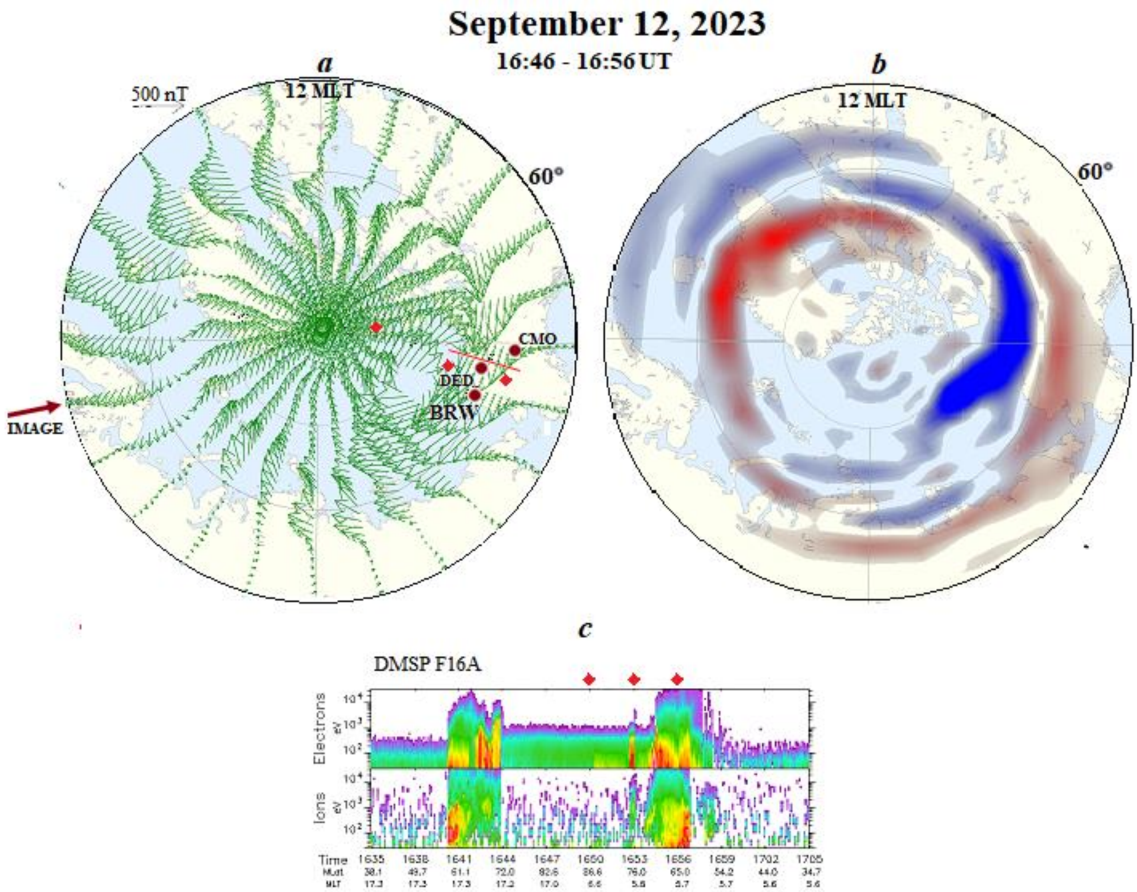

***Figure 6**. AMPERE maps electrojets (a) and field-aligned currents (b) in the maximum of intensity of the substorm in the main phase of the storm; spectrograms of DMSP satellite F16A during the considered interval. Red arrow point the IMAGE meridian, red circles point the location of the station of American sector, red rhombus on the maps mark satellite pass, thin lines show approximate area of particle precipitation measured by F16A.*

Discussion

The similar features were observed during some other *moderate* magnetic storms of the 25th SA cycle. They were characterized by high substorm activity: intense isolated substorms (up to -1000 nT) in the initial phase after a long interval of magnetically quiet conditions and very intense (up to -1500 nT) in the main phase of the storm as one can see in Figure 7. The occurrence of such strong substorms in the main phase of these *moderate* storm looks like similar to the development of supersubstorms – which are typical for much intense magnetic storms [e.g., Hajra et al., 2016; Despirak et al., 2019].

This contradicts the previously published in [Feldstein et al., 1997] a linear relationship between the intensity of the storm and substorms in the storm main phase This result was based on the assumption that the negative IMF *Bz* is the main driver of magnetic disturbances. But now the solar wind dynamic pressure is generally accepted as the second important driver particularly during the periods of the negative IMF *Bz* [Tsurutani and Zhou, 2003; Li and Peng, 2013 and references therein].

Really, our study demonstrated an emerging of substorm activity under the strong negative IMF *Bz* and gradual increase of the solar wind dynamic pressure.

However, the role of the solar wind pressure enhancement in the substorm generation is not sufficiently studied. For example, Sinha et al. [2023] believes that "scenario of substorm onset is simple when the southward component of IMF is present prior to the onset or when just a pressure pulse coincides with the onset. It may be a complex task to understand the behavior of substorm when both the triggering agents are present."

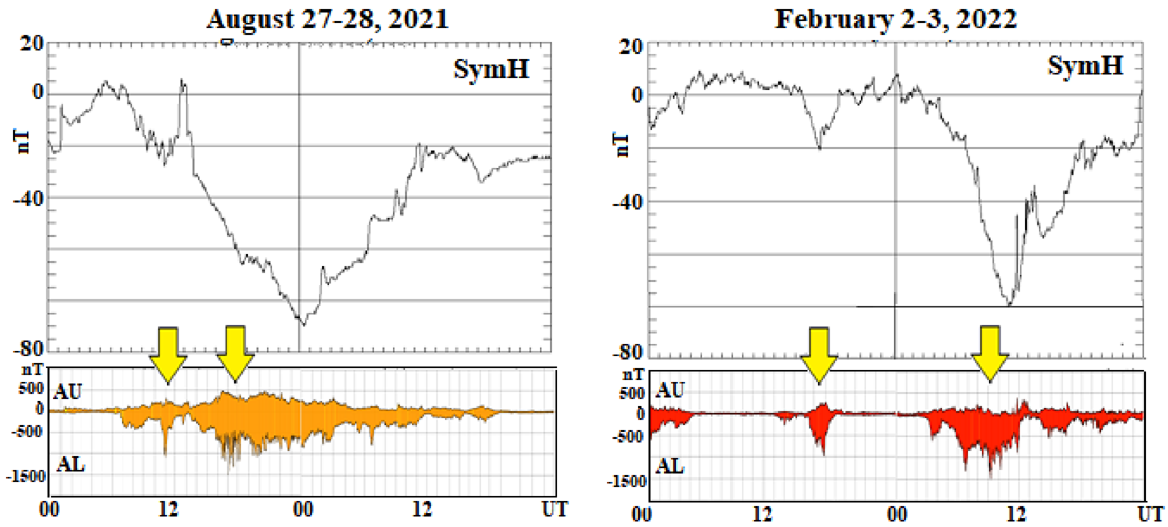

***Figure 7**. Moderate storms of 25th cycle of the solar activity which are characterized by high substorm activity in the initial and main phases of the storm. Substorms are pointed by yellow arrows.*

Conclusion

The spatio-temporal distribution of substorm activity was studied during one of the typical *moderate* magnetic storms, as the most expected storm in the near future.

One of main feature of such storms is the appearance of fairly intense substorms, despite the relatively small values of the intensity of the ring current that is shown by *Dst*- (*SymH*-) index.

The scenario of substorms developed in the main phase of a considered *moderate* storm is similar to the scenario of very intense substorms and supersubstorms, which are typical for storms of much higher intensity.

We assume that the solar wind dynamic pressure plays an important role in the development of substorm under the southward *Bz* component of IMF.

References

Akasofu, S.-I, Chapman, S. (1963). The development of the main phase of magnetic storms, J. Geophys. Res., Vol. 68, pp. 125–129, https://doi.org/10.1029/jz068i001p00125

Despirak, I.V., Lyubchich, A.A., Kleimenova, N.G. (2019). Supersubstorms and conditions in the solar wind, Geomagn. Aeron., Vol. 59, pp. 170–176, https://doi.org/10.1134/S0016793219020075

Feldstein, Y. I., Grafe, A., Gromova, L. I., Popov, V. A. (1997). Auroral electrojets during geomagnetic storms, J. Geophys. Res., Vol. 102, pp. 14223–14235, https://doi.org/10.1029/97JA00577

Gopalswamy, N. et al. (2023). Intense Geomagnetic Storms during Solar Cycles 23-25, Proceedings of the Fifteenth Workshop "Solar Influences on the Magnetosphere, Ionosphere and Atmosphere", pp. 47-55, https://doi.org/10.31401/WS.2023.proc

Hajra, R., Tsurutani, B.T., Echer, E., Gonzalez, W.D., Gjerloev, J.W. (2016). Supersubstorms (SML < -2500nT): Magnetic storm and solar cycle dependences, J. Geophys. Res, Vol. 121, No. 8, pp. 7805-7816, https:/doi.org/10.1002/2015JA021835

Ishkov, V.N. (2023). Medium-Sized Solar Cycles in Different Epochs of Solar Activity, Geomagn. Aeron., Vol. 63, pp. 1024–1030, https://doi.org/10.1134/S0016793223070101

Kepko, L., McPherron, R. L., Amm, O., Apatenkov, S., Baumjohann, W., Birn, J., Lester, M., Nakamura, R., Pulkkinen, T. I., Sergeev, V. (2015). Substorm current wedge revisited, Space Sci. Rev., Vol. 190, pp. 1–46, https://doi.org/10.1007/s11214-014-0124-9

Li, H., Wang, C., Peng, Z. (2013). Solar wind impact on growth phase duration and substorm intensity. J Geophys Res Vol. 118, pp. 4270–4278, https ://doi.org/10.1002/jgra.50399

Selvakumaran, R., Veenadhari, B., Akiyama, S., Pandya, M., Gopalswamy, N., Yashiro, S., Kumar, S., Mäkelä, P. and Xie, H. (2016). On the reduced geoeffectiveness of solar cycle 24: A moderate storm perspective, J. Geophys. Res. Space Physics, Vol. 121, pp. 8188–8202, https://doi.org/10.1002/2016JA022885

Sinha, S., Vichare, G., Sinha, A.K. (2023). Comparative analysis of the role of interplanetary magnetic field (IMF) and sudden impulse (SI) in triggering a substorm. Advances in Space Research, Vol. 71, No. 1, pp. 97-114, https://doi.org/10.1016/j.asr.2022.08.037

Tsurutani, B. T., & Zhou, X.-Y. (2003). Interplanetary shock triggering of substorms: WIND and POLAR. Advances in Space Research, Vol. 31, No. 4, pp. 1063–1067, https://doi.org/10.1016/S0273-1177(02)00796-2